On the interactions between the critical dimensionless numbers associated with multiphase flow in 3D porous media

Ming Fan[1], Laura E. Dalton[2], James McClure[3], Nino Ripepi[1], Erik Westman[1], Dustin Crandall[2], and Cheng Chen[1]

[1] Department of Mining and Minerals Engineering, Virginia Tech, Blacksburg, VA ; [2] National Energy Technology Laboratory, Morgantown, West Virginia; [3] Advanced Research Computing, Virginia Tech, Blacksburg, VA

Abstract

In order to advance the fundamental understanding of multiphase flow in complicated, three dimensional (3D) porous media, the interactions between the critical dimensionless numbers associated with multiphase flow, including contact angle, viscosity ratio, and capillary (Ca) number, were investigated using X-ray micro computed tomography (micro-CT) scanning and lattice Boltzmann (LB) modeling. In this study, the 3D pore structure information was extracted from micro-CT images and then used as interior boundary conditions in a pore-scale LB simulator to simulate multiphase flow within the pore space. A Berea sandstone sample was scanned in three sections using NETL's Geoimaging Lab facilities, and then two-phase flow LB simulations were performed on each section. The LB-simulated water/CO2 distributions agreed well with the micro-CT scanned images, which validated the capability of the LB method in simulating multiphase flow in 3D porous media. Simulation results showed that a decreasing contact angle causes decrease in wetting fluid relative permeability and increase in non-wetting fluid relative permeability. A rising Ca number increases both wetting and non-wetting fluid relative permeabilities, because the higher inertial force favors the mobility of both fluids. An increasing viscosity ratio facilitates the increase of non-wetting fluid relative permeability and mitigates the reduction of wetting fluid relative permeability, when the contact angle decreases continuously.

Results

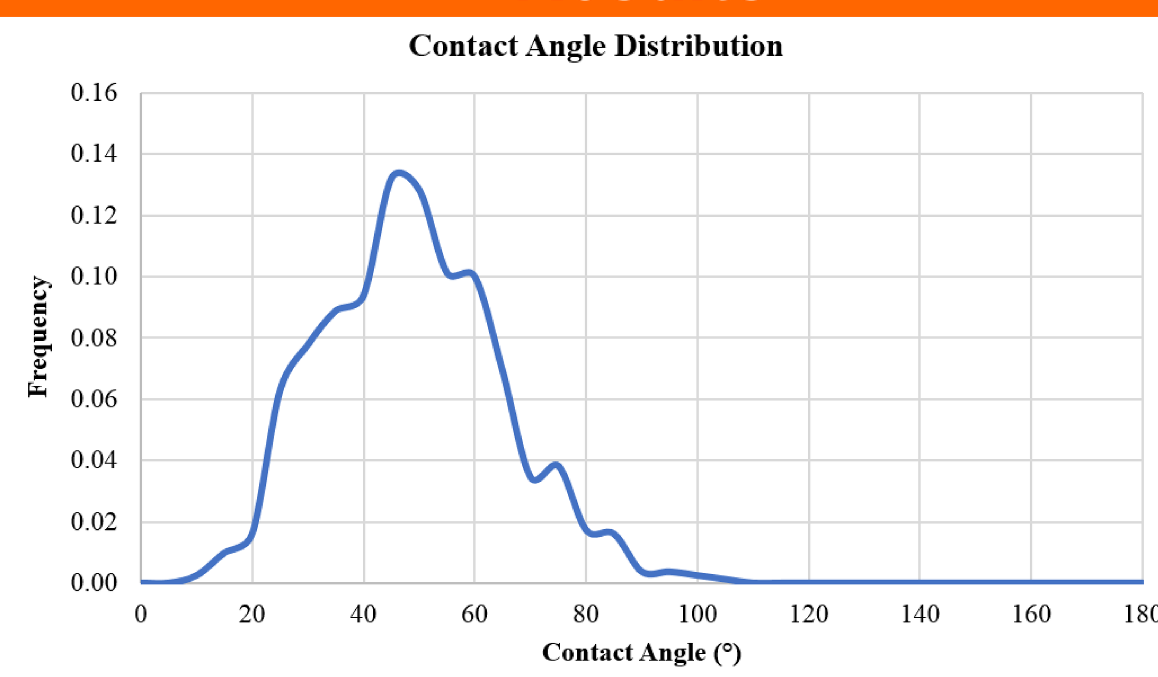

Figure 1. Contact angle distribution at the pore scale measured directly from micro-CT scanning

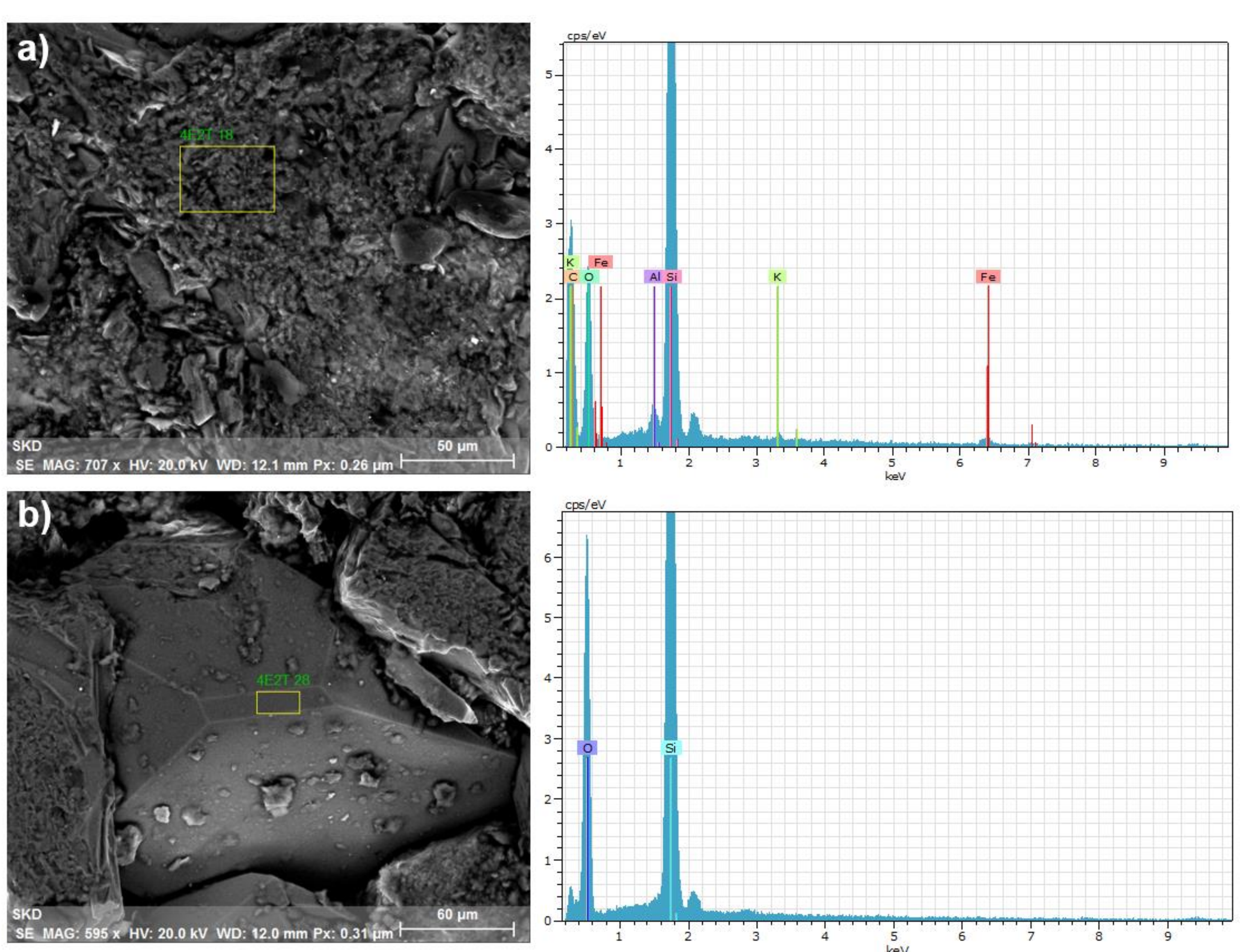

Figure 2. SEM/EDX characterization of sandstone surface rich in a) clay minerals, and b) quartz

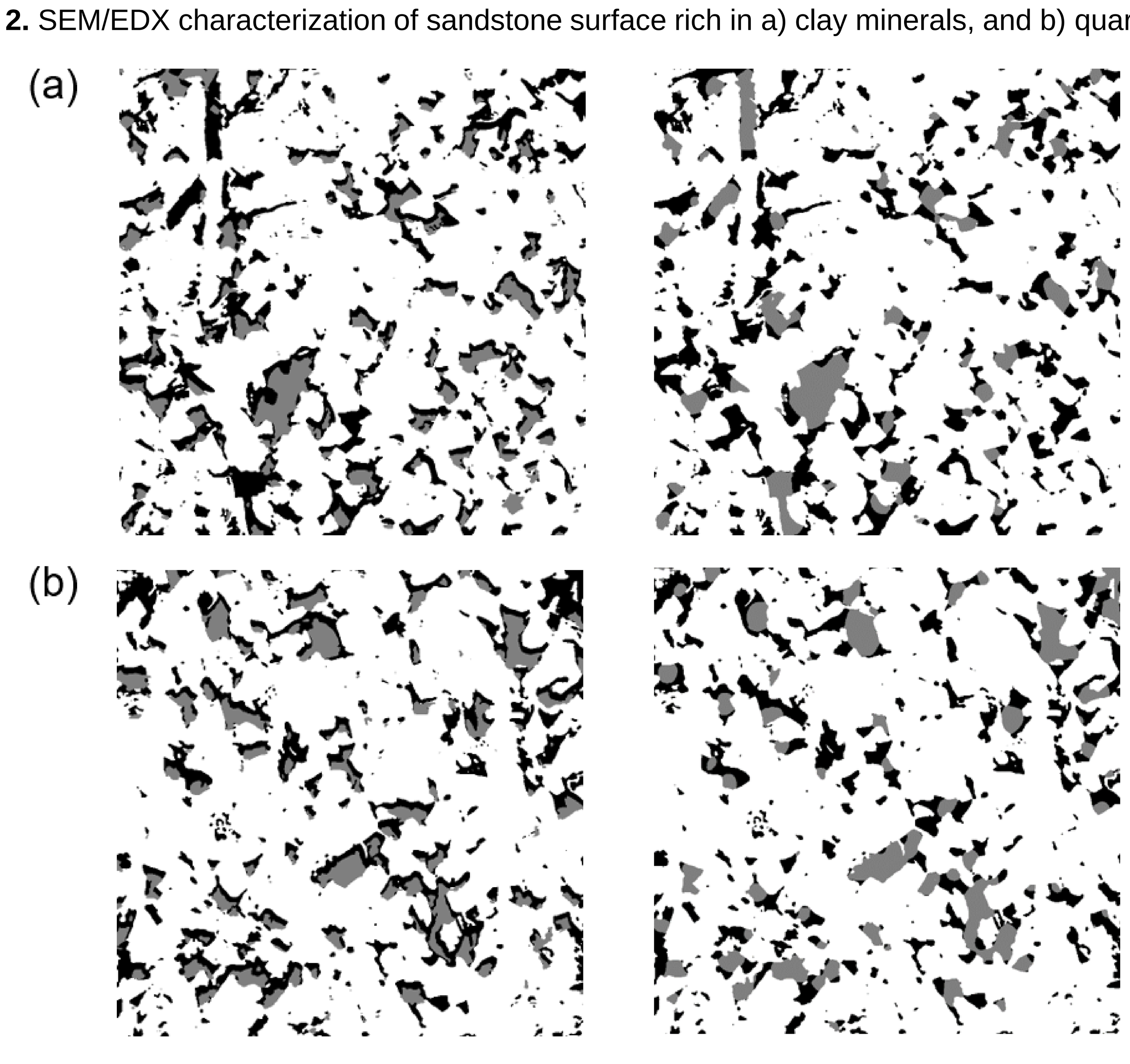

CT-scanned CO_2 (gray) distribution LB-simulated CO_2 (gray) distribution

Figure 3. 2D, horizontal cross sections cut from the 3D image data set of the middle-section computational domain. Distances from the 2D slices to the bottom of the computational domain are a) 0.32 mm, b) 0.75 mm. The left panels are the CT images of two-fluid distribution in the sandstone, and the right panels are the corresponding LB-simulated two-fluid distribution. The water (brine) is black, CO_2 is gray, and sandstone is white. Each picture is a 2D cross section perpendicular to the main-flow (z) direction and has dimensions of 1.89 mm × 1.89 mm

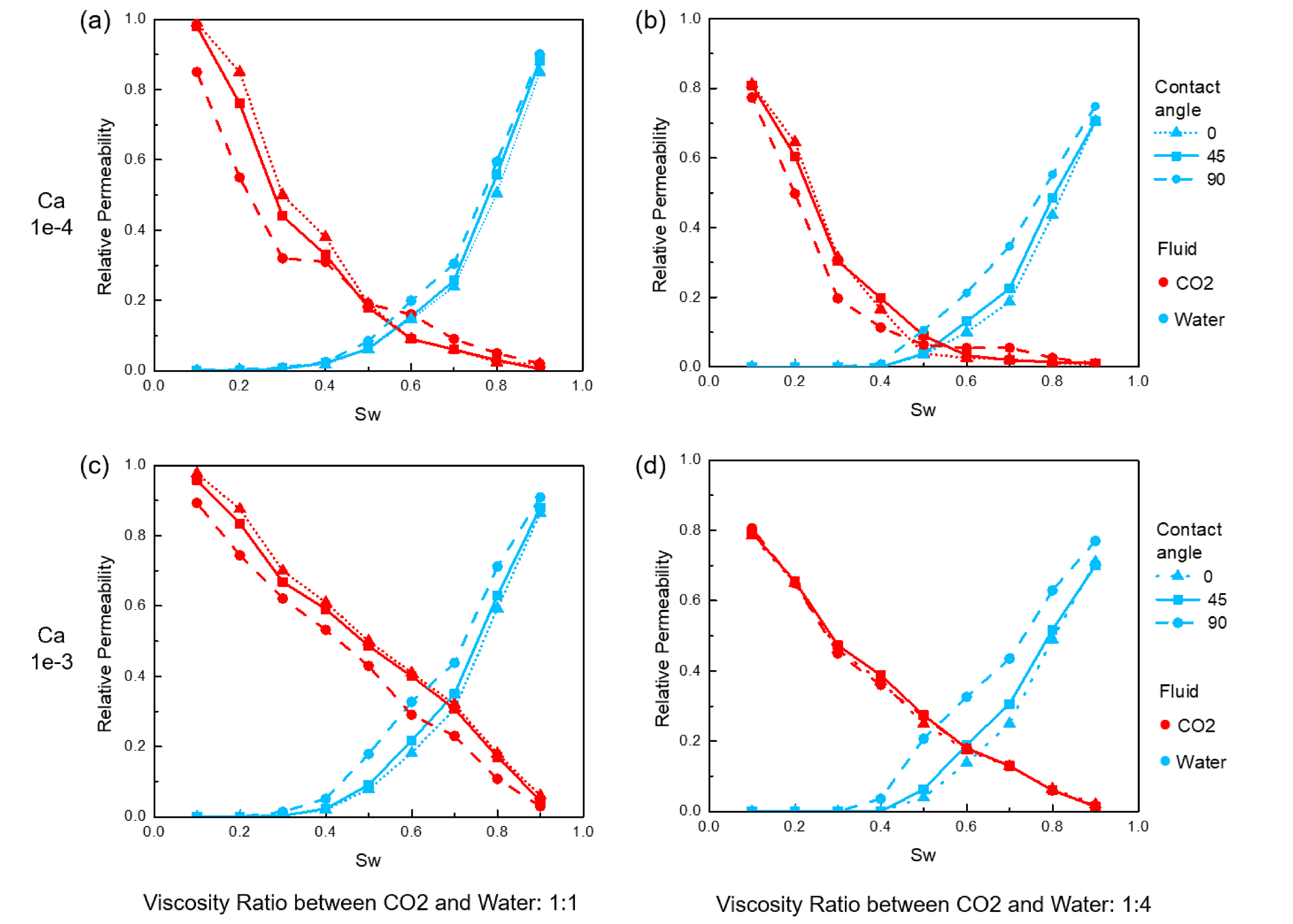

Figure 4. Relative permeability vs. wetting fluid saturation (S_w) curves under two Ca numbers (Ca=1×10^{-4} and Ca=1×10^{-3}) and two viscosity ratios (M=0.25 and M=1). Contact angles of 0°, 45°, and 90° were simulated for each combination of Ca number and viscosity ratio. The computational domain was based on the middle section of the Berea sandstone sample

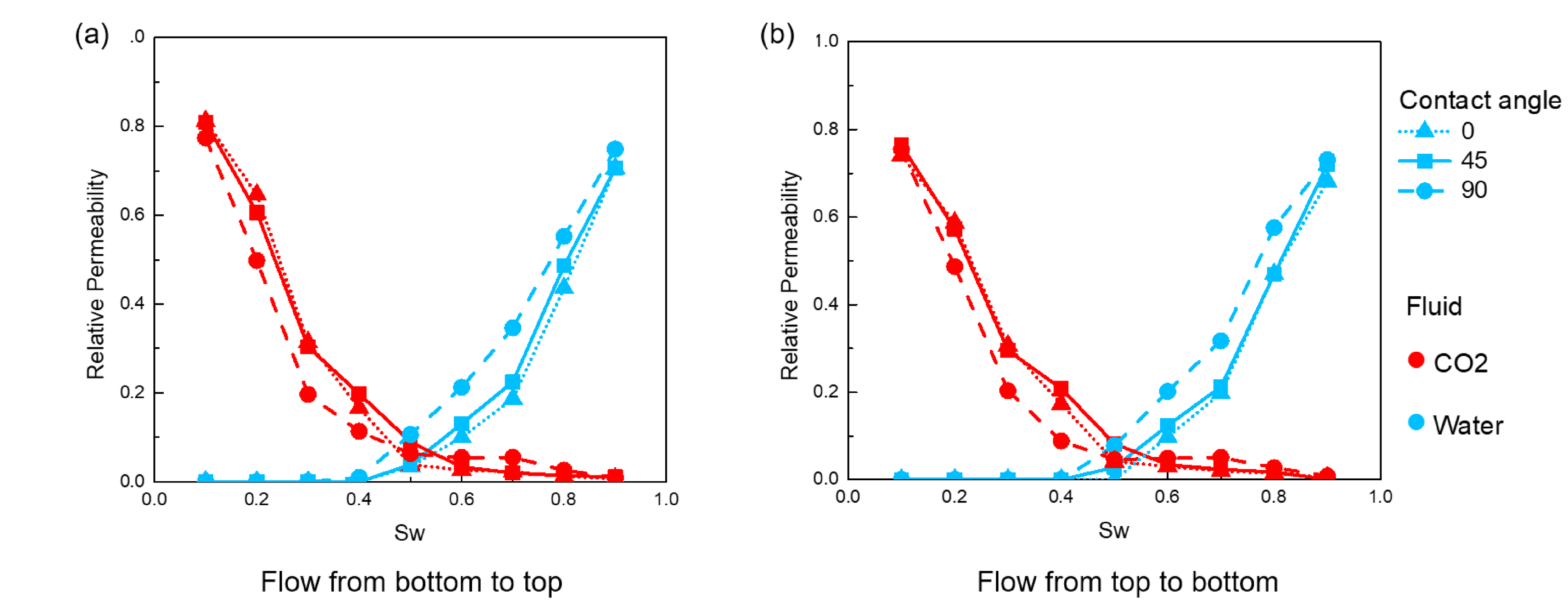

Figure 5. Relative permeability vs. wetting fluid saturation (S_w) curves for fluid injection directions of (a) from bottom to top (in the z direction), and (b) from top to bottom (in the –z direction). The simulations were run on the middle-section computational domain with Ca=1×10^{-4} and M=0.25

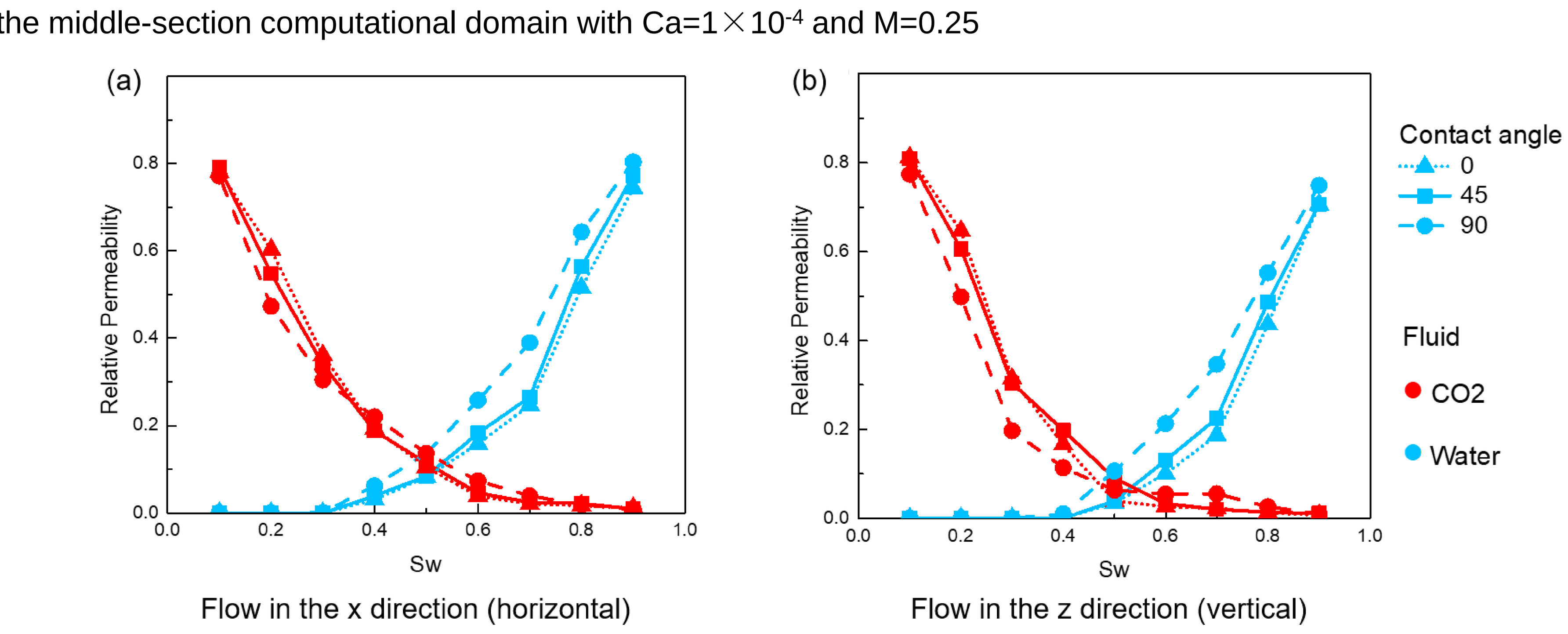

Figure 6. Relative permeability vs. wetting fluid saturation (S_w) curves for fluid injection in the (a) x direction, and (b) z direction. The simulations were run on the middle-section computational domain with Ca=1×10^{-4} and M=0.25

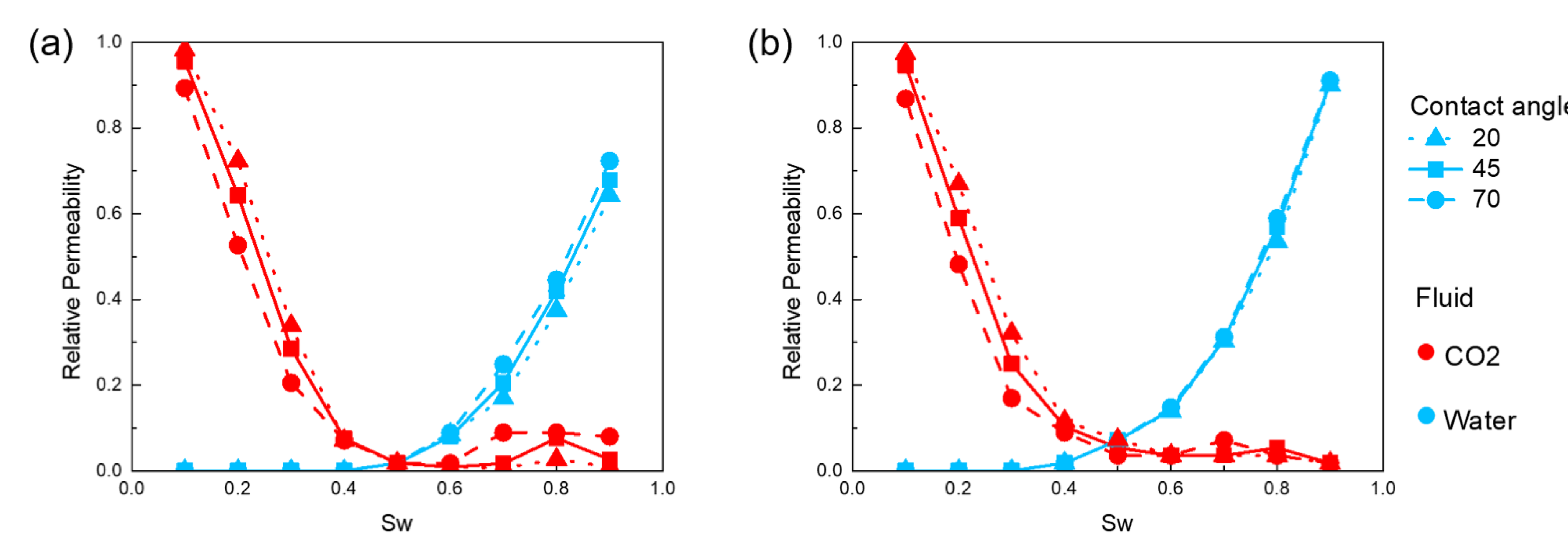

Figure 7. Relative permeability vs. wetting fluid saturation (S_w) curves in the (a) top-section, and (b) bottom-section computational domains. In the simulations, Ca=1×10^{-4} and M=1

Acknowledgements

The authors acknowledge the support of the Junior Faculty Award from Virginia Tech's Institute for Critical Technology and Applied Science and the computational resources from Virginia Tech's Advanced Research Computing Center. The authors are also thankful to the partial support from the National Energy Technology Laboratory Research Participation Program, sponsored by the U.S. Department of Energy and administered by the Oak Ridge Institute for Science and Education.